Biomedicine & Pharmacotherapy 140 (2021) 111765

Contents lists available at ScienceDirect

Biomedicine & Pharmacotherapy

journal homepage: www.elsevier.com/locate/biopha

Original article

Xenocoumacin 2 reduces protein biosynthesis and inhibits inflammatory and angiogenesis-related processes in endothelial cells

Pelin Erkoc [a,b], Michaela Schmitt [a], Rebecca Ingelfinger [a,b], Iris Bischoff-Kont [a], Larissa Kopp [b,e], Helge B. Bode [b,c,d], Susanne Schiffmann [b,e], Robert Fürst [a,b,*]

[a] Institute of Pharmaceutical Biology, Faculty of Biochemistry, Chemistry and Pharmacy, Goethe University Frankfurt, Frankfurt, Germany
[b] LOEWE Center for Translational Biodiversity Genomics (LOEWE-TBG), Frankfurt, Germany
[c] Molecular Biotechnology, Department of Biosciences, Goethe University Frankfurt, Frankfurt, Germany
[d] Max-Planck-Institute for Terrestrial Microbiology, Department of Natural Products in Organismic Interactions, Marburg, Germany
[e] Fraunhofer Institute for Translational Medicine and Pharmacology (ITMP), Frankfurt, Germany

ARTICLE INFO

Keywords:
Natural products
Xenocoumacin
Endothelial cells
Leukocytes
Inflammation
Angiogenesis
Protein biosynthesis

Chemical compounds studied in this article:
Xenocoumacin 1 (PubChem CID: 163752)
Xenocoumacin 2 (PubChem CID: 129089)
Cycloheximide (PubChem CID: 6197)
Staurosporine/ Staurosporin (PubChem CID: 44259)
Celecoxib (PubChem CID: 2662)
Dimethyl Sulfoxide (PubChem CID: 679)
Lipopolysaccharide (PubChem CID: 1970143)
O-Propargyl-Puromycin (PubChem CID: 71576433)

ABSTRACT

Xenocoumacin (Xcn) 1 and 2 are the major antibiotics produced by the insect-pathogenic bacterium *Xenorhabdus nematophila*. Although the antimicrobial activity of Xcns has been explored, research regarding their action on mammalian cells is lacking. We aimed to investigate the action of Xcns in the context of inflammation and angiogenesis. We found that Xcns do not impair the viability of primary endothelial cells (ECs). Particularly Xcn2, but not Xcn1, inhibited the pro-inflammatory activation of ECs: Xcn2 diminished the interaction between ECs and leukocytes by downregulating cell adhesion molecule expression and blocked critical steps of the NF-κB activation pathway including the nuclear translocation of NF-κB p65 as well as the activation of inhibitor of κBα (IκBα) and IκB kinase β (IKKβ). Furthermore, the synthesis of pro-inflammatory mediators and enzymes, nitric oxide (NO) production and prostaglandin E_2 (PGE_2), inducible NO synthase (iNOS), and cyclooxygenase-2 (COX-2), was evaluated in leukocytes. The results showed that Xcns reduced viability, NO release, and iNOS expression in activated macrophages. Beyond these anti-inflammatory properties, Xcn2 effectively hindered pro-angiogenic processes in HUVECs, such as proliferation, undirected and chemotactic migration, sprouting, and network formation. Most importantly, we revealed that Xcn2 inhibits *de novo* protein synthesis in ECs. Consequently, protein levels of receptors that mediate the inflammatory and angiogenic signaling processes and that have a short half-live are reduced by Xcn2 treatment, thus explaining the observed pharmacological activities. Overall, our research highlights that Xcn2 exhibits significant pharmacological in vitro activity regarding inflammation and angiogenesis, which is worth to be further investigated preclinically.

1. Introduction

Natural products, also called secondary products/metabolites, are compounds produced by most microorganisms, fungi, and plants, and are not directly participating in the essential functions of life but rather provide a long-term survival advantage. They have important ecological roles in protecting against predators and competitors as well as in interactions in symbiotic relationships by acting as antibiotics, toxins, or signaling molecules [1,2].

Natural products and their derivatives have been applied by humans to fight diseases and have become important resources for uncovering new therapeutics [3]. For example, nematode-associated bacteria have been evaluated as a potential source of antibiotics. In this symbiotic life cycle, the bacteria defend nematodes against predators and assure the

Abbreviations: ANOVA, analysis of variance; COX-2, cyclooxygenase-2; DMSO, dimethyl sulfoxide; EC, endothelial cell; E-selectin, Endothelial-selectin; FCS, fetal calf serum; HUVEC, human umbilical vein endothelial cells; ICAM-1, intercellular adhesion molecule 1; LPS, lipopolysaccharide; NF-κB, nuclear factor kappa-light-chain-enhancer of activated B cells; NO, nitric oxide; IL-1β, interleukin 1-beta; IκBα, inhibitor of κBα, IKK, IκB kinase; PGE2, prostaglandin E2; iNOS, nitric oxide synthase; PBS, phosphate-buffered saline; TNF, tumor necrosis factor; Xcn, xenocoumacin; VCAM-1, vascular cell adhesion molecule 1.

* Correspondence to: Institute of Pharmaceutical Biology, Faculty of Biochemistry, Chemistry and Pharmacy, Goethe University Frankfurt, Max-von-Laue-Str. 9, 60438 Frankfurt, Germany.
E-mail address: fuerst@em.uni-frankfurt.de (R. Fürst).

https://doi.org/10.1016/j.biopha.2021.111765
Received 9 March 2021; Received in revised form 14 May 2021; Accepted 20 May 2021
Available online 28 May 2021

generation of juveniles [4–6]. Xenocoumacins (Xcns) (Fig. S1), which are water-soluble peptide antimicrobial compounds, are one of the most abundant antibiotics produced by the Gram-negative bacterium *Xenorhabdus nematophila* for its defense. Xcns are structurally related to amicoumacin antibiotics [7], and in their biosynthesis pathway, they are initially produced as an inactive precursor and then cleaved to form active xenocoumacin 1 (Xcn1). Subsequently, this compound is converted to xenocoumacin 2 (Xcn2) to protect the organisms itself from its activity [8,9].

Xcn1 was shown to exhibit a broad antibacterial activity against Gram-positive and -negative bacteria and numerous fungal species, whereas Xcn2 is less active against bacteria and has no activity on the examined fungal species [10,11]. Although Xcns were first discovered as antimicrobial compounds, they were later found to show antiulcer activity: Both forms of the compounds reduced stress-induced gastric ulcers in rats, and, interestingly, Xcn2 displayed a better activity [12]. Nevertheless, no definitive mechanism on the nature of Xcn-induced antiulcer activity was reported. In this regard, Xcns stand out to be investigated as interesting new drug lead compounds.

Inflammation and angiogenesis are involved in various chronic diseases, such as Crohn's disease, rheumatoid arthritis, diabetes, and cancer [13]. Many studies have affirmed the interconnection between endothelial cells (ECs) and leukocytes in the conditions related to the development of pathogenetic processes [14]. The endothelium is activated after exposure to different stimuli, such as infectious and non-infectious agents as well as tissue damage, which alters the internal vascular surface so that it recruits leukocytes and initiates and maintains the inflammatory responses. Besides, ECs migrate and proliferate and thus form new vessels for tissue regeneration once exposed to pro-angiogenic stimuli, which are usually secreted during inflammation by specialized immune cells including macrophages [15]. Deciphering the intricate and interdependent relationships between ECs and leukocytes is important to introduce novel therapeutic approaches.

The influence of Xcns on the EC-leukocyte interaction process has not been explored so far. Hence, in the present study, we aimed to investigate the pharmacological potential of Xcns. An in vitro systematic top-down approach using functional and biochemical assays was followed to determine the mechanism of action of Xcns on the pro-inflammatory EC activation processes as well as on the release of pro-inflammatory mediators and the expression of their synthesizing enzymes in macrophages. Moreover, we aimed to explore the effects of Xcns on in vitro key stages of angiogenesis in human primary ECs, such as proliferation, migration, tube/network, and sprout formation. Our findings show for the first time that Xcns hinder inflammation- and angiogenesis-related processes without causing toxic effects in ECs. In summary, this study underlines the pharmacological potential of Xcn2 regarding inflammatory and angiogenic processes. Altogether, Xcn2 is worth further preclinical characterization.

2. Materials and methods

2.1. Reagents

Xcn1 and Xcn2 (Fig. S1) are produced in *Xenorhabdus* strains, isolated and identified by their characteristic fragmentation patterns, as described previously [16]. In this study, stock solutions of Xcns were prepared by dissolving in DMSO (Sigma-Aldrich, Schnellendorf, Germany). DMSO concentrations on cells did not exceed 0.1% (v/v).

2.2. Cell culture

Primary human umbilical vein endothelial cells (HUVECs) were isolated from human umbilical cords according to Jaffe et al. [17]. The human microvascular endothelial cell line CDC/EU.HMEC-1 (HMEC-1) was obtained from the Centers for Disease Control and Prevention (CDC, Atlanta, GA, USA). Both primary HUVECs and the HMEC-1 cell line were cultured in collagen G (Biochrom AG, Berlin, Germany)-coated 75 cm^2 flasks in supplemented EC growth medium (ECGM) (PELOBiotech, Martinsried, Germany) supplemented with 10% fetal calf serum (FCS) (Biochrom AG), 100 U/ml penicillin, 100 μg/ml streptomycin, and 2.5 μg/ml amphotericin B (PAN-Biotech, Aidenbach, Germany), and a supplement mixture (PELOBiotech). HUVECs were used for experimental purposes exclusively in passage three. RAW264.7 murine macrophages were obtained from the American Type Culture Collection (ATCC), and the human monocytic-like cell line THP-1 was purchased from the German Collection of Microorganisms and Cell Cultures GmbH (DSMZ). These two cell lines were cultured in RPMI1640 medium (PAN-Biotech) supplemented with 10% heat-inactivated FCS, 100 μg/ml streptomycin, and 100 U/ml penicillin. All cells were incubated at 37 °C in an atmosphere of 5% CO_2 and 95% air.

2.3. Metabolic activity assay

A CellTiter-Blue cell viability assay (Promega GmbH, Mannheim, Germany) was performed to analyze the influence of Xcns on the metabolic activity of endothelial cells. In brief, confluent HUVECs were treated with the indicated concentrations of Xcn1 and Xcn2 or DMSO (0.1%) as vehicle control for 24 h. Four hours before the end of the treatment, CellTiter-Blue reagent containing resazurin was added to the cells in a ratio of 1:10. Resazurin is reduced into the fluorescent dye resorufin by viable cells. The metabolic activity was determined by fluorescence measurements (ex: 579 nm, em: 584 nm) using a microplate reader (Tecan Infinite F200 Pro; Tecan, Männedorf, Switzerland).

2.4. Apoptosis assay

Late apoptosis was detected according to the method of Nicoletti et al. [18]. HUVECs were treated as indicated and were incubated overnight in the dark in a PBS solution containing propidium iodide (PI) (50 μg/ml; MilliporeSigma, Darmstadt, Germany), sodium citrate (0.1%; Carl Roth, Karlsruhe, Germany), and Triton X-100 (0.1%; MilliporeSigma) at 4 °C. The percentage of cells with sub-diploidic DNA content was measured using a FACSVerse flow cytometer (BD Biosciences, Heidelberg, Germany). The pan-kinase inhibitor staurosporine (MilliporeSigma) served as a positive control.

The apoptosis assay for RAW264.7 cells was performed as described previously [19]. Briefly, 0.2×10^5 RAW264.7 cells were seeded in a black poly-D-lysine-coated 96-well plate and incubated for 24 h at 37 °C. Xcn1, Xcn2, or vehicle (DMSO) diluted in RPMI1640 medium without phenol red was added to the cells and incubated for 24 h at 37 °C. CellEvent Caspase-3/7 Green Detection (Thermo Fisher Scientific, Waltham, MA, USA) reagent was incubated for 90 min at 37 °C (without CO_2). Afterward, cells were incubated with DRAQ5 (Cy5 channel) for 30 min at room temperature. Images were taken using the ImageXpress Micro Confocal High Content Imaging System (Molecular Devices, San Jose, USA). The fluorescence signal of cell nuclei and apoptotic cells was detected. The percentage of dead cells was determined using the "live/dead"-analysis tool by calculating the ratio of apoptotic cells to all cells using MetaXpress software (Molecular Devices).

2.5. Lactate dehydrogenase (LDH) cytotoxicity assay

The LDH CytoTox 96 Non-Radioactive Cytotoxicity Assay kit (Promega GmbH, Mannheim, Germany) was used according to the manufacturer's instructions [20]. After treating the cells with Xcns for 24 h, supernatants of cells were collected immediately to determine LDH release using a Varioskan Flash plate reader (ThermoFisher Scientific) at 490 nm wavelength.

2.6. Endothelial cell proliferation assay

HUVECs (3000 cells/well) were seeded into collagen-coated 96-well

plates and grown for 24 h. Then, they were treated with a concentration range of Xcn1 and Xcn2. Treated cells were cultured for 72 h, whereas untreated control cells, directly after 24 h, were fixed with a methanol-ethanol (2:1) solution and washed with PBS before they were stained using a crystal violet solution (20% methanol). Similarly, at the end of incubation time, Xcn-treated cells were fixed, stained, and unbound crystal violet was removed by washing with distilled water. Finally, cells were left to air dry, and DNA-bound crystal violet was dissolved using acetic acid solution (20%, Sigma-Aldrich). Absorbance was measured at 590 nm using a plate reader (Tecan Infinite F200Pro, Tecan). The proliferation percentage was calculated by normalizing to the untreated control (24 h) and compared to the DMSO control (0.03%) of 72 h incubation.

2.7. Cytotoxicity assay on RAW264.7 cells

The cytotoxicity assay was performed as described previously [19]. Briefly, 0.2×10^5 RAW264.7 cells were incubated for 24 h at 37 °C. The cells were treated with increasing concentrations of Xcn1 and Xcn2 or vehicle (DMSO) for 24 h, and viability of cells was detected with the WST-8 reagent (Orangu™, HiSS Diagnostics, Freiburg, Germany). The assay was accomplished as recommended by the supplier. The absorbance was measured at 440 nm and 600 nm (reference) using an EnSpire Plate Reader (PerkinElmer, Waltham, MA, USA). The absorbance at 440 nm was normalized to the absorbance at 600 nm. The sample values were corrected with the background wells (wells with medium and without cells). The absorbance of the treated samples was related to the control sample and the control was set to 100%.

2.8. Adhesion of leukocytes to endothelial cells

The adhesion of leukocytes to ECs under flow conditions was analyzed using μ-slides $I^{0.8}$Luer (Ibidi, Martinsried, Germany) and an Ibidi Pump System, as described previously [21]. HUVECs (1.6×10^6 cells/ml) were seeded into μ-slides and cultured for 24 h with a continuous flow of 5 dyn/cm^2. Then, they were preincubated with Xcn2 for 30 min and activated with TNF (10 ng/ml) or IL-1β (5 ng/ml) for 24 h. For the leukocyte adhesion assay, untreated THP-1 cells (8×10^5 cells/ml) were stained with CellTracker Green (Thermo Fisher Scientific) and were allowed to adhere to the treated HUVECs for 10 min under a flow of 0.5 dyn/cm^2. Non-adherent THP-1 cells were removed through washing steps. Phase-contrast images were taken with an inverted microscope DM IL Light Emitting Diode (Leica Microsystems, Wetzlar, Germany). Later, the fluorescence signal from adherent THP-1 cells was measured after cell lysis using RIPA-buffer by a Tecan Infinite F200 Pro microplate reader (excitation: 485 nm, emission: 535 nm; Tecan).

For the investigation of leukocyte adhesion under static conditions, confluent primary HUVECs or HMEC-1 cells (passage number: 15–20), were treated as explained above. CellTracker Green-labeled THP-1 cells (passage number <30, 1×10^5 cells/ml) and RAW264.7 cells (4×10^4 cells/ml), which were treated with lipopolysaccharide (LPS, 150 ng/ml) for 24 h, were allowed to adhere onto a HUVEC monolayer for 5 and 10 min, respectively. After washing off unadhered cells the fluorescence signal from adherent leukocytes was measured by Tecan Infinite F200 Pro microplate reader (excitation: 485 nm, emission: 535 nm; Tecan).

2.9. Cell surface expression of cell adhesion molecules

The effect of Xcns on the expression of the intercellular adhesion molecule 1 (ICAM-1), vascular cell adhesion molecule 1 (VCAM-1), and E-selectin on the cell surface of endothelial cells was investigated by flow cytometry using fluorescence-labeled antibodies. Anti-CD62E (551145) and anti-CD106 (555647) mouse monoclonal E-selectin and VCAM-1 antibodies, respectively, were obtained from BD Biosciences. Mouse anti-human CD54-FITC (MCA532F) antibody for ICAM-1 was from Bio-Rad (Hercules, CA, USA). HUVECs were grown until confluence and treated as indicated. Then, HUVECs were detached from the plate and incubated with the above-mentioned antibodies according to the manufacturer's instructions, and surface protein levels were measured with a FACSVerse flow cytometer (BD Biosciences).

2.10. Western blot

HUVECs were treated as described. After cell lysis with RIPA buffer, proteins were separated with SDS-PAGE and transferred to a polyvinylidene fluoride membrane (Bio-Rad) using a tank. 5% nonfat dried milk powder (Carl Roth) or BSA was used to block membranes before incubation with primary and secondary antibodies. The following primary antibodies were used: rabbit polyclonal anti-ICAM-1 antibody (sc-107, 1:500), mouse monoclonal anti-VCAM-1 antibody (sc-13160, 1:300), anti-E-selectin antibody (sc-137054, 1:500), anti-NFκB p65 antibody (sc-8008, 1:400), mouse monoclonal anti-EGFR (sc-373746, 1:100) from Santa Cruz Biotechnology (Dallas, TX, USA); anti-inhibitor of κB kinase (IKK)-β antibody (8943, 1:1000), anti-inhibitor of κBα (IκBα) antibody (9242, 1:1000), anti-phosphorylated (phospho)-IKKα/β antibody (2697, 1: 1000), anti-phosphorylated (phospho)-IκBα antibody (2859, 1:1000), and anti-TNF-R1 antibody (3736, 1:1000), rabbit monoclonal anti-VEGFR 2 (9698, 1:2000), rabbit monoclonal anti-VEGFR 1 (64094, 1:1000), rabbit monoclonal anti-FGFR 1 (9740, 1:1000), rabbit monoclonal anti-Akt (4691, 1:1000) and anti-phosphorylated (phospho)-Akt (Ser473) (4060, 1:2000), rabbit polyclonal anti-p44/42 MAPK (Erk1/2) antibody (9102, 1:1000), mouse monoclonal phospho-p44/42 MAPK (Erk1/2, Thr202/Tyr204) antibody (9106, 1:2000) from CellSignaling Technology (Frankfurt am Main, Germany); anti-β-actin antibody (A3854, 1:100,000) from Sigma-Aldrich. Horseradish peroxidase-conjugated secondary antibodies were either anti-mouse antibody (7076, 1:2000) or anti-rabbit antibody (7074, 1:3000) from CellSignaling Technology. Alexa Fluor 488-linked anti-mouse antibody (A11001A, 1:400) was obtained from Thermo Fischer Scientific (Dreieich, Germany). A self-prepared chemiluminescence reagent was used for protein detection. Densitometric analyses were performed by ImageJ software (1.53c).

For protein level analysis of RAW264.7 cells, 1×10^6 cells were seeded in a 6-well plate and preincubated with Xcn1, Xcn2, and vehicle (DMSO) at 37 °C for 1 h, followed by a 24 h stimulation with LPS (100 ng/ml). At the end of incubation time, cells were washed once with cold PBS and harvested. For lysis, the cell pellets were resuspended in RIPA-buffer completed with a protease inhibitor cocktail (Roche complete, Sigma Aldrich, Schnelldorf, Germany). Afterward, cells were sonicated at 60% power for 10 s, and the suspension was centrifuged at 12,000 g at 4 °C for 20 min. The protein concentration was determined with the Bradford method. 100 μg protein lysates were mixed with loading dye, denatured, separated on a 10% acrylamide gel, and blotted to a nitrocellulose membrane. The membrane was incubated with anti-iNOS (13120, 1:500; CellSignaling Technology) for 3 days, with anti-COX2 (12282 S, 1:1000; CellSignaling Technology) overnight and with anti-β-actin (A1978, 1:6000; Sigma-Aldrich) for 1 h. The secondary antibodies (AlexaFlour488 anti-rabbit A11030; 1:10,000 and AlexFlour546 anti-mouse; 1:10,000; Thermo Fischer Scientific were incubated for 1 h. For normalization, β-actin was used as a housekeeping gene.

2.11. Quantitative real-time PCR

HUVECs were grown until confluence and treated as indicated. RNA isolation was performed using the RNeasy Mini Kit (Qiagen, Hilden, Germany) according to the manufacturer's protocol. After cDNA synthesis (SuperScript II Reverse Transcriptase, Thermo Fisher Scientific), the cDNA was mixed with primers and Sybr Green PCR Master Mix (Thermo Fisher Scientific). Quantitative PCR was performed on a StepOnePlus system from Thermo Fisher Scientific. The $2^{-\Delta\Delta Ct}$ method was used for quantification. The following primers were ordered at Eurofins (Germany): ICAM-1 (forward, 5′-CTG CTC GGG GCT CTG TTC-3′;

reverse, 5′-AAC AAC TTG GGC TGG TCA CA-3′), VCAM-1 (forward, 5′-CCA CAG TAA GGC AGG CTG TAA-3′; reverse, 5′-GCT GGA ACA GGT CAT GGT CA-3′), E-selectin (forward, 5′-AGA TGA GGA CTG CGT GGA GA-3′; reverse, 5′-GTG GCC ACT GCA GGA TGT AT-3′), glyceraldehyde 3-phosphate dehydrogenase (forward, 5′-CCA CAT CGC TCA GAC ACC AT-3′; reverse, 5′-TGA AGG GGT CAT TGA TGG CAA-3′); TNF-R1 (forward, 5′-CAA GCC ACA GAG CCT AGA CA-3′; reverse, 5′-GAA TTC CTT CCA GCG CAA CG-3′). The Ct for the gene of interest was normalized to that of glyceraldehyde-3-phosphate dehydrogenase.

For qPCR analysis of RAW264.7 cells, 3×10^5 cells were seeded in a 6-well plate and preincubated with Xcns in the indicated concentrations or vehicle (DMSO) at 37 °C for 1 h, followed by a 24 h treatment with LPS (100 ng/ml). After the incubation time, cells were washed once with cold PBS and harvested. mRNA was isolated with an RNeasy mini kit (Qiagen, Hilden, Germany) and cDNA was synthesized with the first-strand cDNA synthesis kit (Thermo Fisher Scientific) according to the manufacturer's instructions. The following primers (Biomers.net GmbH, Ulm, Germany) were used: muCOX-2 (forward, 5′-AAG ACT ACG TGC AAC ACC TGA G-3′; reverse, 5′-GTG CCA GTG ATA GAG TGT GT-3′), muiNOS (forward, 5′-CCA AGC CCT CAC CTA CTT CC-3′; reverse 5′-CTC TGA GGG CTG ACA CAA GG-3′), muPPIA (forward, 5′-GCT GGA CCA AAC ACA AAC GG-3′; reverse, 5′-GCC ATT CCT GGA CCA AAA C-3′). For the analysis of the mRNA expression, the $2^{-\Delta\Delta Ct}$ method was used. The Ct values of the treated samples were normalized to the Ct values of PPIA and related to the DMSO-treated samples.

2.12. Measurements of nitric oxide and PGE_2 levels

20,000 RAW264.7 macrophages per well were plated in a 96-well cell culture plate and cultured for 24 h at 37 °C. To test if Xcns induce nitric oxide (NO) or prostaglandin E_2 (PGE_2) synthesis, Xcn1 (0.125, 0.25, 0.5 μM), Xcn2 (0.062, 0.0125, 0.25 μM), vehicle (DMSO) and positive control (100 ng/ml; LPS) were added. To test if Xcns inhibit NO or PGE_2 synthesis, the cells were pre-incubated with Xcns, 10 μM celecoxib (Cele, positive control), or control (DMSO) for 60 min before 100 ng/ml LPS was added. After 24 h supernatants were collected and stored at −80 °C.

NO was determined with the Griess method. Briefly, 80 μl cell supernatant or standard sample were added to a 96-well microplate and thereafter, 20 μl sulfanilamide solution (120 mg sulfanilamide (Sigma-Aldrich) in 30 ml 1 N hydrochloric acid) and 20 μl naphthylenediamine solution (180 mg *N*-(1-naphthyl) ethylenediamine dihydrochloride (Carl Roth) in 30 ml water) were added. After 15 min, the absorbance (540 nm) was measured with an EnSpire Plate Reader (PerkinElmer, Waltham, MA, USA). N^G-methyl-L-arginine acetate salt (L-NMMA), which is a non-selective inhibitor of all NOS isoforms [22], was used as a positive control.

PGE_2 was determined using a competitive ELISA from Enzo Life Sciences (Farmingdale, USA). The ELISA was performed according to the manufacturer's protocol. Briefly, anti-PGE_2 antibodies are bound onto the surface of 96-well plates. Test samples and alkaline phosphatase-conjugated PGE_2 were added to the wells. After incubation, the excess reagents were washed away and *p*-nitrophenyl phosphate was added and catalyzed by alkaline phosphatase to produce *p*-nitrophenol, a yellow-colored product, which was detected with EnSpire Plate Reader (PerkinElmer, Waltham, MA, USA). The intensity of the yellow coloration is inversely proportional to the amount of PGE_2.

2.13. Undirected migration assay

Undirected migration of HUVECs was evaluated as previously described [23]. A scratch was generated on a confluent layer of cells in 24-well plates followed by Xcn2 treatment. Then, cells were allowed to migrate for 8 h until the gap was closed in the DMSO-treated control group (representing 100% migration). The relative migration was calculated in relation to the starting point and was analyzed using the ImageJ software (1.53c).

2.14. Chemotactic migration assay

For the evaluation of chemotactic migration of HUVECs, μ-Slide chemotaxis chambers (Ibidi) were used according to the manufacturer's instructions as previously described [23]. Briefly, HUVECs were suspended in the growth medium with a density of 1×10^6 cells/ml, 6 μl of cell suspension was delivered into the channels. After 4 h of incubation for adhesion, the cells were gently washed once with M199 medium (supplemented with 1% FCS and 1% Pen/Strep) to eliminate culture medium and non-adherent cells. Then, HUVECs were treated with 3 μM of Xcn2, while side channels were filled with a stable concentration gradient of FCS (1–20%). The chemotactic migration of cells on slides was observed in a climate chamber (37 °C, 5% CO_2) for 20 h using a Leica DMI6000 B fluorescence microscope (Leica Microsystems). Images of migrating cells were taken every 10 min (121 slices in total) using a 5X air objective. The directionality, Y-forward values, Euclidean and accumulated distances, the velocity, and center of the mass density of the migrated HUVECs were determined using "Manual Tracking" and "Chemotaxis Analysis" plugins of ImageJ (1.53c).

2.15. Spheroid assay

HUVEC spheroids were generated as previously described [23], using the hanging drop method in square Petri dishes. HUVECs (400 cells/drop) were distributed in a culture medium containing methylcellulose (0.25%, Sigma-Aldrich). After 24 h, HUVEC spheroids (~125 spheroids/condition) in methylcellulose solution (with freshly added 10% FCS) were resuspended in collagen I (Corning, rat tail, product number 354236) with a 1:1 ratio and transferred into a 48-well plate at 37 °C. Gels were pretreated with Xcn2 for 30 min and then the sprouting was induced by VEGF (10 ng/ml) (PeproTech EC, London, UK) for 20 h. Microscopical images were taken by using a Leica DM IL LED microscope (Leica Microsystems) and ImageJ (1.53c) was used to determine the total sprout length and the number of sprouts per spheroid.

2.16. Network formation assay

To analyze the effect of Xcn2 on the ability of HUVECs to form tube-like structures, μ-Slide angiogenesis chambers (Ibidi) were used as previously described [23]. The wells were coated with 10 μl ice-cold growth factor reduced Matrigel (Corning) for 45 min at 37 °C. Subsequently, HUVECs (10,000 cells/well) were seeded onto the gel in a 50 μl culture medium without or with Xcn2. Total tube length and the number of junctions were calculated from the analysis of microscopy images using the "Angiogenesis Analyzer" plugin of Image J (1.53c).

2.17. Protein synthesis assay

The Click-iT Plus OPP Alexa Fluor 488 Protein Synthesis Assay Kit (Thermo FisherScientific) was used according to the manufacturer's instructions and as described previously [23]. Briefly, HUVECs were grown in μ-Slides 8-well (ibidi) until confluence and treated as indicated. For the last 30 min of Xcn2 treatment, cells were additionally incubated with 20 μM Click-iT *O*-propargyl-puromycin (OPP) leading to the incorporation of OPP into newly translated proteins. After fixation and permeabilization, the incorporated OPP was labeled with the fluorescent dye Alexa Fluor 488, and microscopical images were obtained using a Leica DMI6000 B fluorescence microscope (Leica Microsystems). The intensity of the Click-iT OPP signal was normalized to the intensity of a cell nuclei staining (NuclearMask Blue Stain) using ImageJ (1.53c).

2.18. Immunofluorescence staining for p65 nuclear translocation

A previously described method was used to visualize p65 nuclear

translocation [21]. Briefly, HUVECs (55,000 cells/well) were seeded on 8-well μ-slides (Ibidi GmbH, Gräfelfing, Germany) and grown to confluence. Then, cells were treated with Xcn2, and at the end of treatment time, they were fixed with 4% Roti-Histofix (Carl Roth, Karlsruhe, Germany). Afterward, cells were permeabilized with 0.2% Triton X-100 (Sigma Aldrich). After blocking of unspecific binding sites with 0.2% BSA in PBS, the cells were incubated with an anti-NFκB p65 antibody (sc-327, 1:400; Santa Cruz Biotechnology, Heidelberg, Germany) and subsequently with an Alexa Fluor 488-conjugated secondary antibody (A11008, 1:400; Thermo Fisher Scientific, Dreieich, Germany). Fluorescence images were taken using a Leica DMI6000 B fluorescence microscope (Leica Microsystems). Images were analyzed with the ImageJ (1.53c).

2.19. Statistical analysis

All data were statistically analyzed using the GraphPad Prism software version 6 (GraphPad, San Diego, USA). One-way ANOVA followed by Tukey's post hoc test was used to analyze all bar graphs. As an exception, an unpaired *t*-test was used in the chemotactic migration assay. The numbers of independently performed experiments (n) are stated in the corresponding figure captions, and at least three technical replicates were used for the experiments, except the western blot analysis, adhesion assay under flow, protein synthesis, and chemotaxis assays. The Rayleigh test was used to test the uniformity of a circular distribution of points in chemotactic migration assay, and the null hypothesis is rejected when $P > 0.05$. All data are expressed as mean ± standard error of the mean (SEM). $P \leq 0.05$ was considered as statistically significant.

3. Results

3.1. Xcns do not impair endothelial cell viability

First, non-toxic ranges of Xcn1 and Xcn2 were determined in HUVECs. The metabolic activity, cell membrane integrity, and sub-

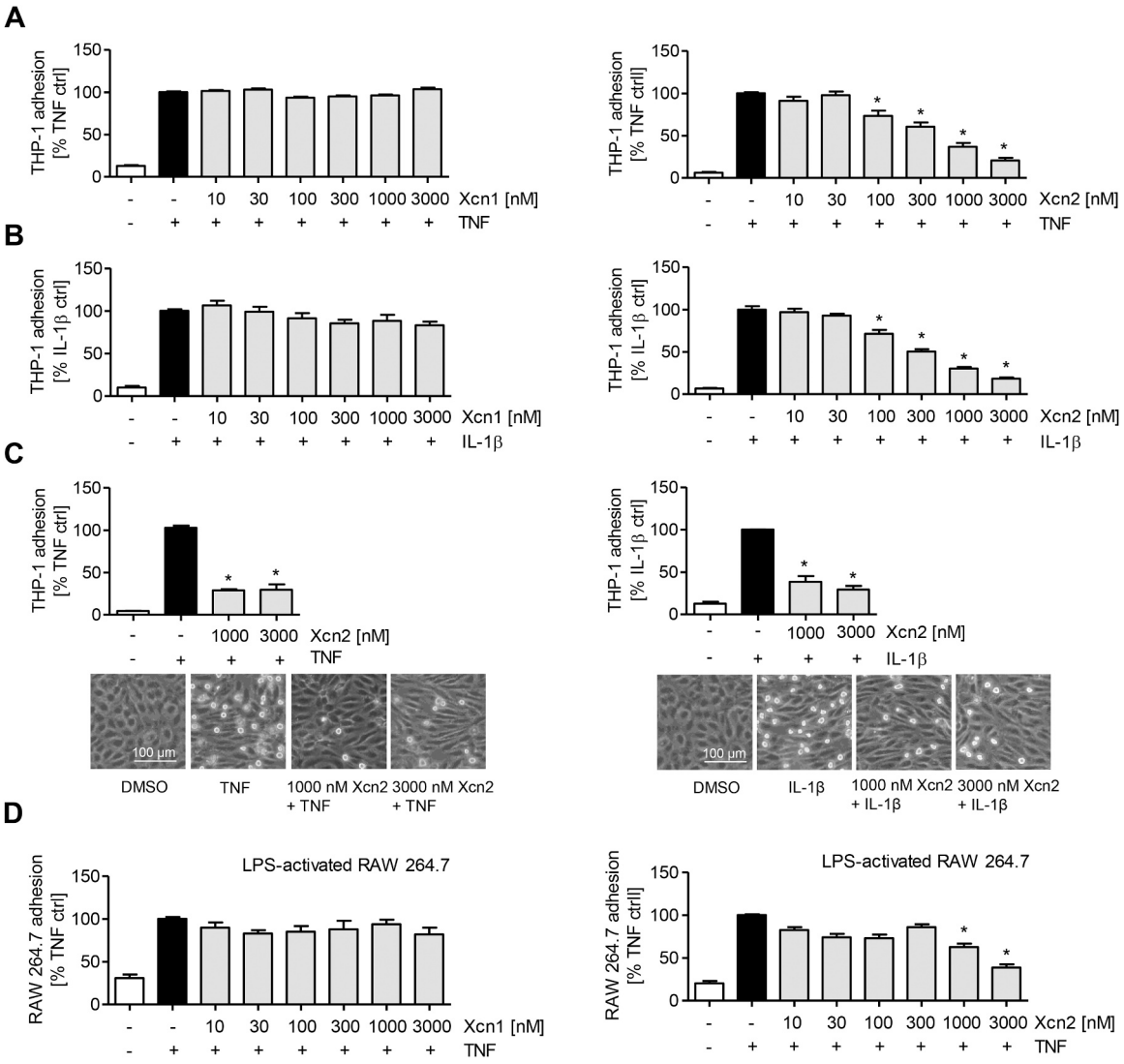

Fig. 1. Xcn2 reduces the adhesion of leukocytes on endothelial cells. (A-B) THP-1 cell adhesion under static conditions. HUVECs were grown to confluence, preincubated with Xcn1 (left) or Xcn2 (right) for 30 min and activated with (A) TNF (10 ng/ml) or (B) IL-1β (5 ng/ml) for 24 h. For the leukocyte adhesion assay, untreated THP-1 cells were stained with CellTracker Green and were allowed to adhere onto the treated HUVECs for 5 min (C) THP-1 cell adhesion under flow conditions. HUVECs were grown under the cultivation flow of 5 dyn/cm^2 for 24 h, preincubated with Xnc2 for 30 min, and activated with (left) TNF (10 ng/ml) or (right) IL-1β (5 ng/ml) for 24 h. (D) RAW264.7 cell adhesion under static conditions was induced by TNF on Xcn1 (left) and Xcn2 (right) treated cells. The adhesion of leukocytes onto ECs was quantified by fluorescence measurements for all cell adhesion experiments. Data are expressed as means ± SEM, n = 3. *$P \leq 0.05$ vs. TNF (positive) control.

diploid (apoptotic) populations were analyzed by the CellTiter-Blue assay (Fig. S2A), lactate dehydrogenase (LDH) quantification (Fig. S2B), and flow cytometry using propidium iodide (PI) staining (Fig. S2C), respectively. As indicated by these three test systems, there was no significant cytotoxicity of Xcns on HUVECs at concentrations up to 3 μM for 24 h.

3.2. Xcn2 reduces adhesion of leukocytes onto endothelial cells

The extravasation of leukocytes from the blood into the inflamed tissue is a key step of the body's inflammatory response, and the adhesion of leukocytes onto the vascular endothelium is a crucial prerequisite for this extravasation [24]. Therefore, we first tested Xcns for their ability to reduce the adhesion of human monocytic (THP-1) cells onto a TNF- or IL-1β-activated EC monolayer under static conditions: As shown in Fig. 1A, B, Xcn2 treatment of HUVECs significantly diminished both the TNF- and IL-1β-induced THP-1 cell adhesion starting from a concentration of 100 nM. In contrast, Xcn1 had no effect. The adhesion of THP-1 cells was further examined under flow conditions using the most effective concentrations (Fig. 1C): THP-1 adhesion was decreased by more than 50% compared to the positive control group. In addition to macrovascular HUVECs, THP-1 cell adhesion was significantly decreased when microvascular HMECs were treated with Xcn2 under static conditions starting from 100 nM (Fig. S3). To explore this effect with a different leukocyte cell line, we used RAW264.7 macrophages (Fig. 1D). While Xcn1 treatment of HUVECs did not alter RAW264.7 cell adhesion, Xcn2 lowered cell adhesion starting from 1000 nM.

3.3. Xcn2 down-regulates the expression of endothelial CAMs

To investigate the effect of Xcns on the levels of CAMs, which are crucially engaged in the adhesion of leukocytes onto ECs, we screened for inhibition of the TNF- and IL-1β-induced expression of the CAMs. Xcn2 exerted a significant inhibitory activity in TNF-induced HUVECs on cell surface protein levels of ICAM-1, VCAM-1, and E-selectin, starting at a concentration of 100 nM (Fig. 2A), as well as total protein levels starting from 300 nM (Fig. 2A). Xcn2 also reduced total protein levels of ICAM-1, VCAM-1, and E-selectin in IL-1β-activated HUVECs in a concentration-dependent manner (Fig. S4B). In addition to the protein levels of CAMs, we also measured the mRNA expression of these molecules by q-RT-PCR. mRNA expression of the CAMs was significantly increased by Xcn2 treatment in TNF- (Fig. 2C) and IL-1β-activated HUVECs (Fig. S4B). Only an exceptional decrease of VCAM-1 levels was observed at 3000 nM.

3.4. Xcn2 down-regulates key modulators of the canonical NF-κB pathway

Considering the influence of Xcn2 on endothelial CAMs, which are predominantly regulated by the NF-κB pathway, we focused on the signaling molecules that are crucially involved in the activation cascade of this transcription factor. The first step was to investigate the action of Xcn2 on the TNF-induced translocation of the NF-κB subunit p65 from the cytosol into the nucleus, which was visualized by immunofluorescence staining. The translocation was significantly reduced after 24 h treatment with Xcn2 when cells were activated with TNF for a short period (up to 30 min) (Fig. 3A). However, there was no significant difference between Xcn2 treated and untreated cells when longer periods of activation with TNF (1–3 h) were used (Fig. 3B). In contrast, there was an increase in IL-1β-mediated translocation of p65 by Xcn2 (Fig. S5A, B).

For the activation of NF-κB, the degradation of IκB proteins is of importance. This arises mainly from the activation of the IκB kinase (IKK) complex [25]. By Xcn2 treatment for 6 h, TNF-mediated phosphorylation of IκBα was strongly inhibited (Fig. 3C). IKK-β is responsible for the phosphorylation of IκBα, which is followed by the proteasomal degradation of IκBα, a necessity for the nuclear translocation of the NF-κB subunit p65 [21,26]. The TNF-evoked phosphorylation of IKK-β was reduced up to approximately 50% (Fig. 3D). The reduction in the TNF-mediated phosphorylation of IkBα and IKK-β was still present after 24 h treatment with Xcn2 (Fig. S5C, D). Besides, the influence of Xcn2

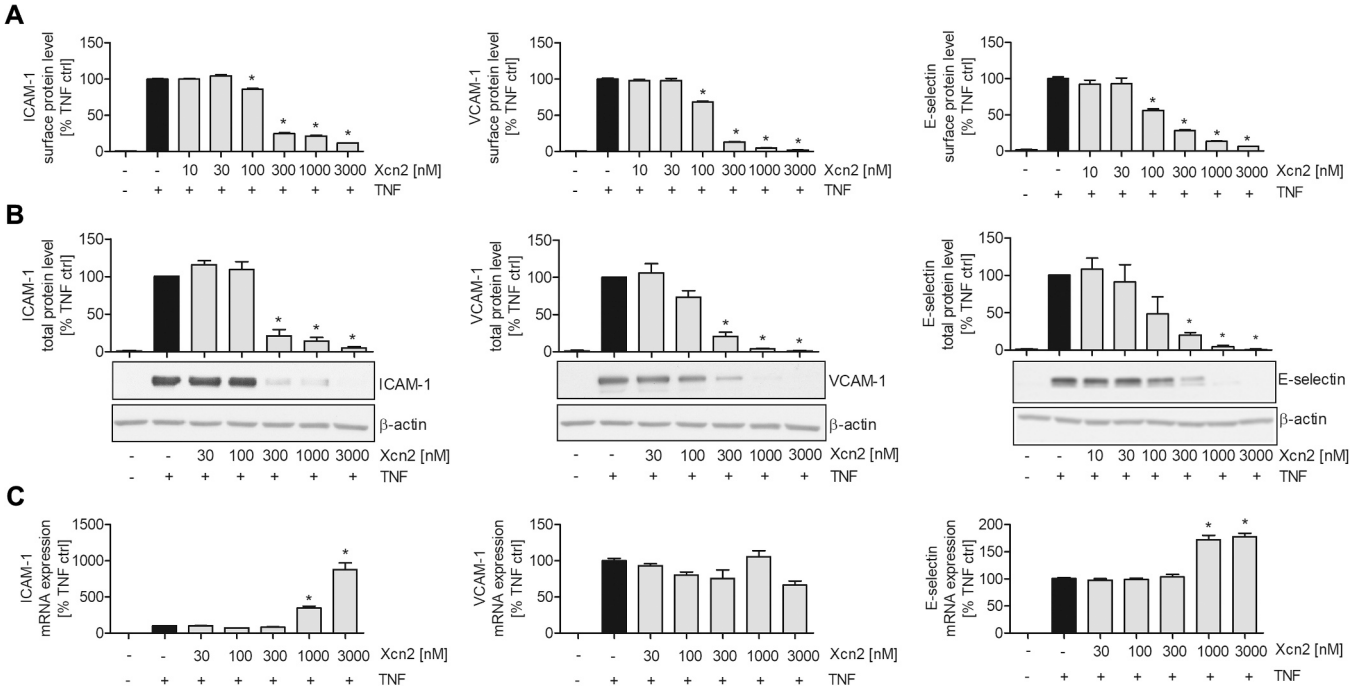

Fig. 2. Xcn2 down-regulates the expression of endothelial CAMs. Confluent HUVECs were left untreated (control) or were pretreated with Xcn2 for 30 min and were then activated with TNF (10 ng/ml) for 24 h (ICAM-1 and VCAM-1) or 4 h (E-selectin). (A) Surface protein levels were analyzed by flow cytometry. (B) Total protein expressions were analyzed by Western blot analysis. One representative blot out of 3 independently performed experiments is shown. (C) mRNA expression was determined by q-RT-PCR. Data are expressed as means ± SEM, n = 3. *$P \leq 0.05$ vs. TNF control.

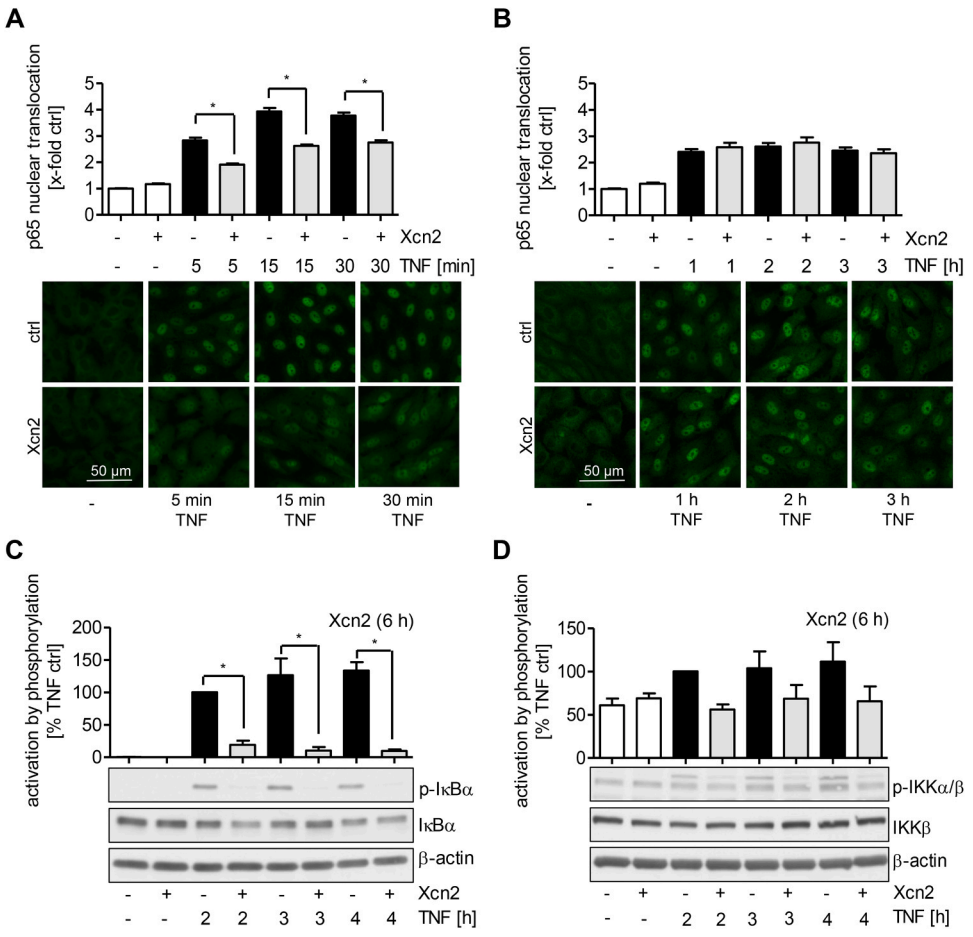

Fig. 3. Xcn2 blocks the nuclear translocation of p65 and influences the phosphorylation of IκBα and IKKα/β. (A, B) p65 translocation into the nucleus was determined by immunocytochemistry and fluorescence microscopy by analyzing the nuclear fluorescence intensity (green). Confluent HUVECs were pretreated with Xcn2 (1000 nM) for 30 min and activated with TNF (10 ng/ml) as indicated for (A) shorter and (B) longer periods. Total protein levels of (C) IκBα and phospho-IκBα (p-IκBα) (**D**) IKKβ, phospho-IKKα/β (p-IKKα/β), and β-actin were analyzed by western blot. Confluent HUVECs were treated with Xcn2 (1000 nM) for 6 h and activated with TNF (10 ng/ml). One representative blot out of 3 is shown. Data are expressed as mean ± SEM. (A, B) n = 3, (C, D) n = 5, * $P \leq 0.05$ versus control.

on the IL-1β-evoked increase in the phosphorylation of IκBα and IKK-β was not as strong as the action of Xcn2 on the TNF-induced events (Fig. S5E, F). Xcn2 induced an IL-1β-mediated decrease in p-IκBα protein level after 4 h of treatment (Fig. S5E).

3.5. Xcns reduce cell viability, NO release, and iNOS expression in RAW264.7 macrophages

Besides ECs, we were also interested in the action of Xcns on the pro-inflammatory activation of RAW264.7 macrophages. First, the half-maximal inhibitory concentration (IC_{50}) values on RAW macrophages were determined with a cell proliferation reagent, WST-8, as 610 and 240 nM for Xcn1 and Xcn2, respectively (Fig. 4A). Then, the apoptosis level of Xcn-treated cells was detected by measuring caspase-3 activation (Fig. 4B). Even though caspase-3 levels were slightly augmented with increasing concentrations of Xcn1 and Xcn2, these compounds augmented the levels up to only 10%, while the positive controls celecoxib (Cele) and staurosporine (STS) strongly induced apoptosis up to approximately 90%.

Next, we investigated if the Xcns affect the synthesis of two main inflammatory mediators in macrophages, nitric oxide (NO) and prostaglandin E_2 (PGE_2). The concentrations of NO and PGE_2 were determined from the supernatant of LPS-induced RAW264.7 cells. Neither Xcn1 nor Xcn2 did alter PGE_2 level in LPS-activated macrophages (Fig. 4C). The LPS-induced NO level was decreased with increasing concentrations of Xcn1 and Xcn2 (Fig. 4D).

Furthermore, the effects of Xcns on COX-2 and iNOS mRNA and protein levels were analyzed in LPS-induced RAW macrophages. The COX-2 mRNA level was significantly higher in Xcn2-treated cells compared to Xcn1-treated and untreated cells, and this increase was concentration-dependent (Fig. 4E). In line with the NO release results, mRNA levels of iNOS also decreased with increasing concentrations of Xcns, and Xcn2 exhibited a slightly stronger activity in decreasing iNOS mRNA levels than Xcn2 (Fig. 4F). Regarding the total protein levels, we found that COX-2 in RAW macrophages was not significantly affected by Xcn1 and Xcn2 (Fig. 4G). On the other hand, iNOS protein levels were decreased by Xcn1 and Xcn2 treatment in RAW264.7 cells, whereby Xcn1 exerted a stronger effect than Xcn2.

3.6. Xcn2 impedes angiogenic processes in HUVECs

As a next step, we examined the effects of Xcns on angiogenic key features in vitro. Essential stages in the process of angiogenesis, i.e., proliferation, migration, sprouting, and network formation, were evaluated.

The proliferation of HUVECs was assessed by measuring the number of crystal violet-stained cells. Although we found out that the viability of HUVECs was not influenced by Xcns, the proliferation was hindered upon treatment with Xcn1 and Xcn2 for 72 h (Fig. 5A). Xcn2 decreased the proliferation starting from a concentration of 100 nM, whereas Xcn1 was only effective at the highest concentration used (3000 nM). We also observed that Xcn2 exhibited similar effectiveness at 24 and 48 h treatment, while Xcn1 was able to reduce proliferation at 3000 nM only after 48 h of treatment (Fig. S6).

To assess the effects of Xcns on the undirected migration of HUVECs, a scratch assay was performed. Xcn2 but not Xcn1 significantly reduced

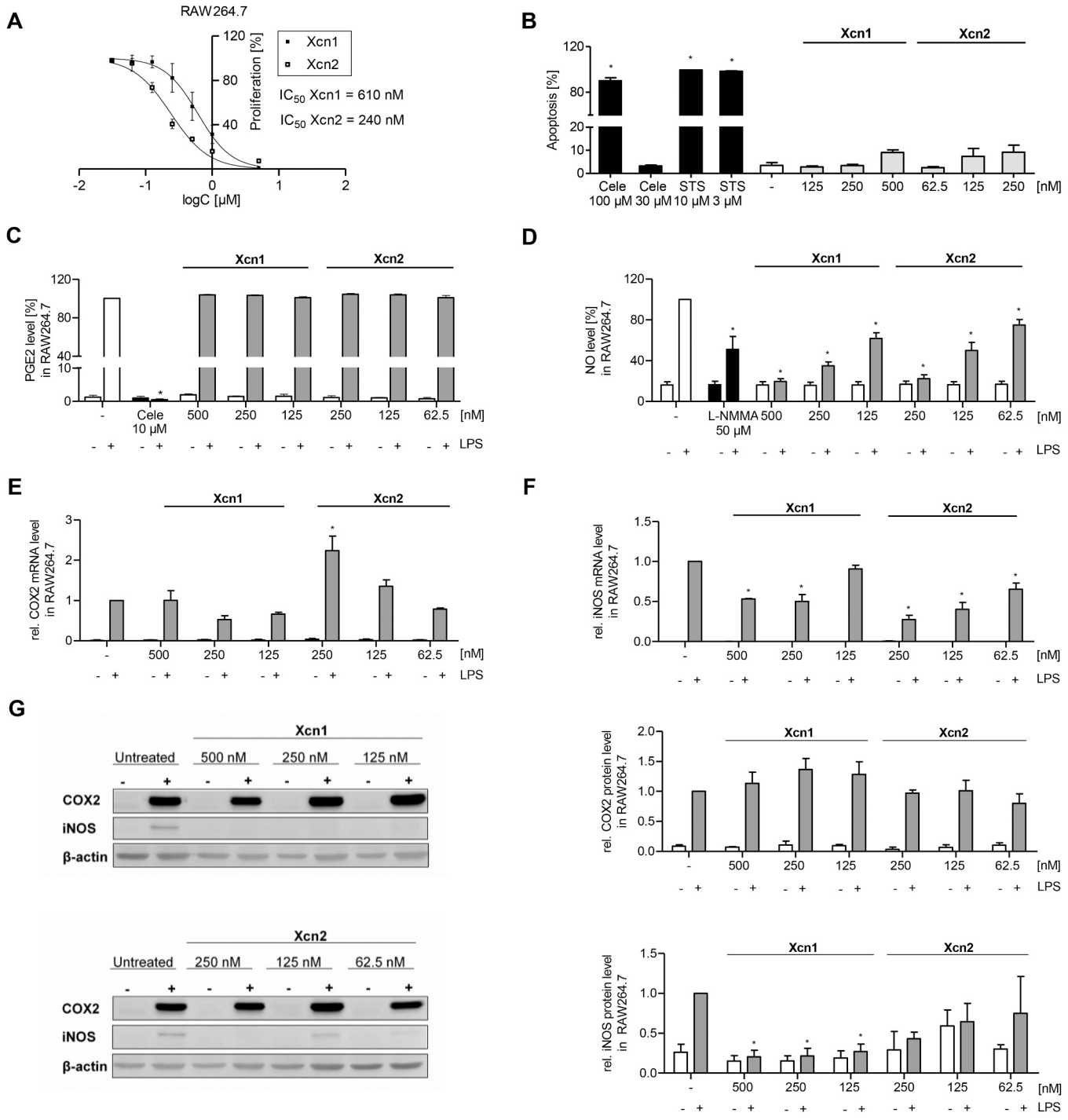

Fig. 4. Influence of Xcns on RAW macrophages. (A) IC_{50} determination from proliferation assays. RAW 264.7 cells were incubated with Xcns or DMSO (control) for 24 h. WST-8 dye was added for 60 min and formazan was quantified. (B) Apoptosis assay. RAW 264.7 cells were incubated with Xcns or DMSO for 24 h. Apoptotic cells were stained with a caspase-3-detecting antibody. Determination pro-inflammatory activation, (C) PGE2, (D) NO release. RAW macrophages were preincubated with Xcns or DMSO (control) for 30 min followed by the addition of 100 ng/ml LPS for 24 h. (E) mRNA expressions of COX-2 and (F) iNOS, (G) protein level of COX-2 and iNOS. RAW264.7 cells were preincubated with Xcns and DMSO at 37 °C for 1 h, followed by a 24 h stimulation with LPS (100 ng/ml). Data are expressed as mean ± SEM. n = 3, * $P \leq 0.05$, treatment groups versus vehicle control for (A-B); treatment groups versus vehicle control with LPS (C-G).

the migration of cells (Fig. 5B, Fig. S7). After confirming the superiority of Xcn2 in reducing endothelial proliferation and migration, the following experiments were performed with Xcn2 only. To determine the influence of Xcn2 on the migratory capability of HUVECs towards a chemotactic stimulus, a live-cell imaging experiment using stable FCS gradients was performed. The chemotactic migration of cells treated with Xcn2 (3000 nM) was imaged for 20 h. The distribution homogeneity of migrated cells was statistically confirmed by the Rayleigh test. Xcn2 treatment resulted in a significant reduction in the displacement of Y-forward migration of cells, and the center of mass of HUVECs (Fig. 5C). Also, the directionality and Euclidean distance between the start and completion points of the tracking paths were significantly decreased. The accumulated distance and velocity were not diminished compared to FCS control. In addition, angiogenic sprouting

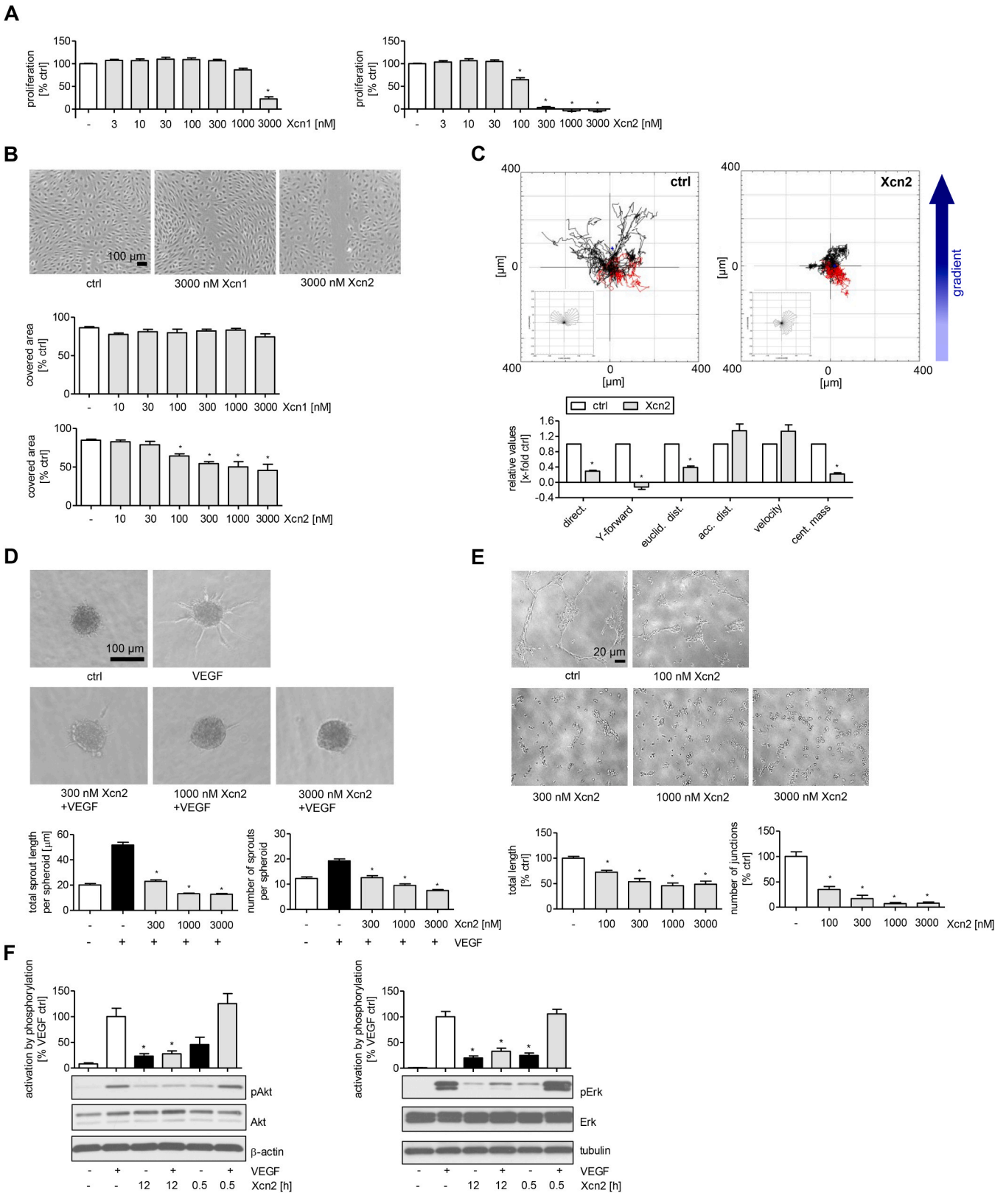

(caption on next page)

Fig. 5. Xcn2 inhibits angiogenic processes in HUVECs. (A) Proliferation assays. HUVECs were grown in low-density and treated with Xcn1 (left) and Xcn2 (right) for 72 h. Cells were stained with crystal violet solution. The amount of DNA-bound crystal violet was detected by absorbance measurements. (B) Undirected migration (wound healing). A scratch was formed on a HUVEC monolayer using a pipette tip. The cells were incubated in a growth medium or growth medium containing the indicated concentrations of Xcn1 and Xcn2 and allowed to migrate for 8 h followed by fixation and microscopical analysis. (C) Live-cell microscopic analysis of chemotactic migration. Chemotaxis of HUVECs towards a serum gradient (20% FCS) was determined under control conditions (DMSO) and in the presence of Xcn2 (3000 nM) in μ-Slide Chemotaxis chambers (ibidi). Cell movements were tracked for 20 h. (D) VEGF-induced angiogenic sprouting from endothelial cell spheroids. The hanging drop method was used to form HUVEC spheroids, followed by the seeding of spheroids in a collagen gel after 24 h, and spheroids were pretreated with Xcn2 for 30 min and sprouting was induced by VEGF (10 ng/ml) for 20 h. (E) Formation of endothelial networks. HUVECs were seeded on growth factor reduced Matrigel and treated with the indicated concentrations of Xcn2. (F) The effects of Xcn2 on the activation of Akt and Erk1/2 proteins. Confluent HUVECs were starved in growth factor reduced medium for 12 h, followed by the treatment with Xcn2 (1000 nM) or left untreated before the activation with VEGF (10 ng/ml) for 5 min, and the protein levels pan and phosphorylated forms of Akt and Erk1/2 (left to right) were evaluated by western blot analysis. ImageJ was used to analyze cell movements, cell sprouts and network formation, and band density of western blots. Data are expressed as mean ± SEM. n = 3, * $P \leq 0.05$ versus DMSO control (A, B, E), FCS (C) or VEGF control (D, F).

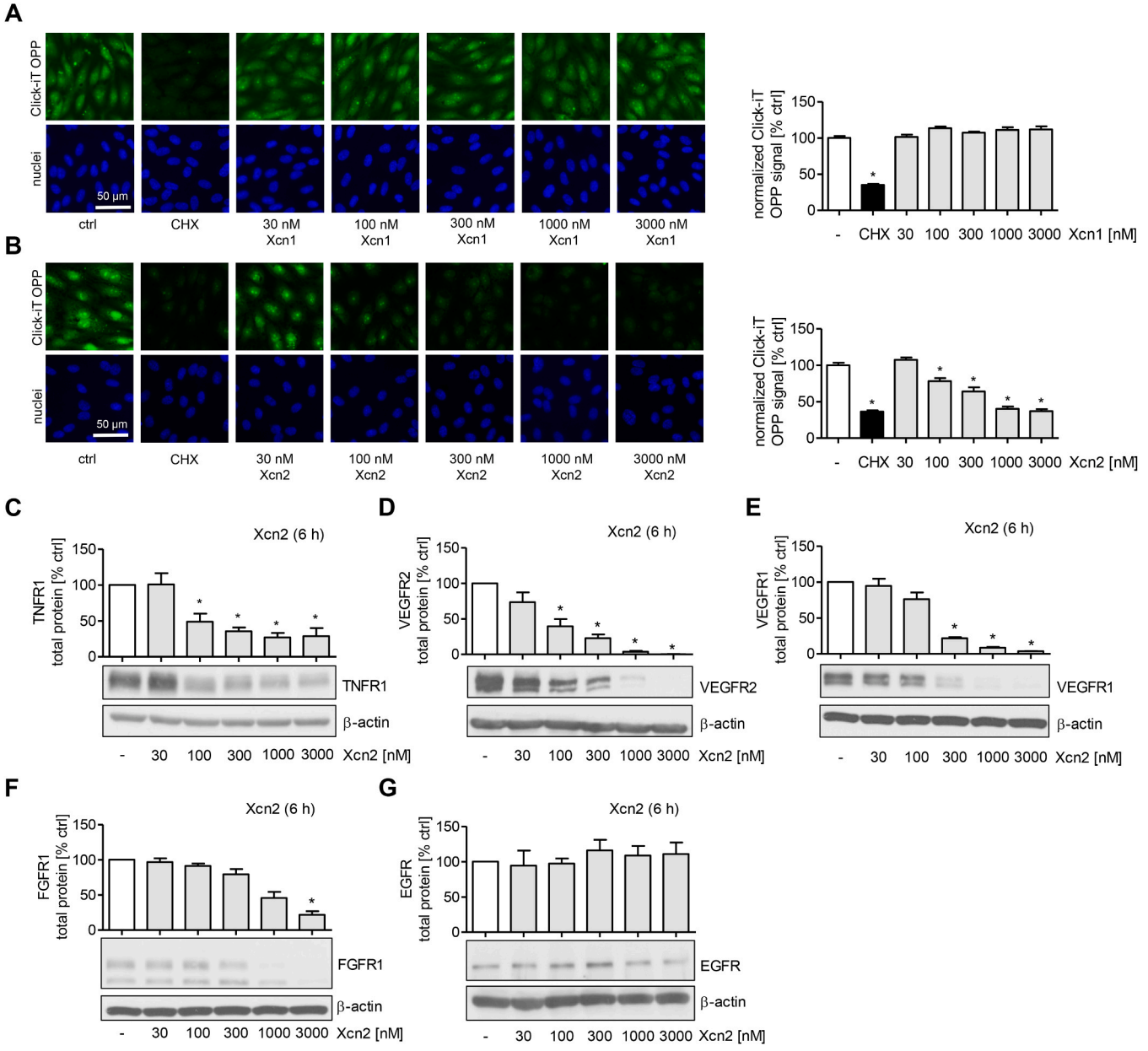

Fig. 6. Xcn2 influences the surface protein levels by blocking the *de novo* protein biosynthesis of HUVECs. Confluent HUVECs were treated with (A) Xcn1 and (B) Xcn2 in different concentrations or cycloheximide (CHX; 10 μg/ml) for 6 h. For the last 30 min of Xcn treatment, the cells were incubated with Click-iT OPP, which was fluorescently labeled with Alexa Fluor 488. Microscopical images were obtained and the intensity of the Click-iT OPP signal (green) was normalized to the intensity of a cell nuclei staining (blue) using ImageJ. The total protein levels of human (C) tumor necrosis factor receptor 1 (TNFR1), (D) vascular endothelial growth factor receptor 2 (VEGFR2), (**E**) vascular endothelial growth factor receptor 1 (VEGFR1), (**F**) fibroblast growth factor receptor-1 (FGFR1), and (**G**) epidermal growth factor receptor (EGFR) was obtained from confluent HUVECs, which were treated with a concentration range of Xcn2 for 6 h as indicated. ImageJ was used to analyze the band density of western blots. Data are expressed as mean ± SEM. n = 3, * $P \leq 0.05$ versus control.

from spheroids and endothelial tube/network formation was blocked in the presence of Xcn2 as shown in Fig. 5D, E. Xcn2 (starting from 300 nM) impeded the increase in the VEGF-induced total sprout length and the number of sprouts. Moreover, in the tube/network formation assay the total tube length and number of junctions were analyzed from microscopy images. As shown in Fig. 5E, the reducing effect of Xcn2 on the total tube length starts at a concentration of 100 nM and is constant between 300 and 3000 nM. Besides, Xcn2 decreased the number of junctions in the EC network by more than 50% for the indicated concentrations.

Finally, we hypothesized that Xcn2 might alter the protein levels of key regulators of angiogenesis. Further tests showed that the treatment of ECs with Xcn2 for 12 h reduces the VEGF-induced activation (phosphorylation) of two key protein kinases that regulate the angiogenic response: Akt and ERK1/2, [27,28] as shown in Fig. 5F. The total protein level of these proteins stayed constant upon Xcn2 treatment.

3.7. Xcn2 inhibits protein biosynthesis in HUVECs

The effects of Xcn2 on the *de novo* protein biosynthesis were measured using an *O*-propargyl-puromycin-based assay. As shown in Fig. 6A and B, Xcn2 reduced protein synthesis in a concentration-dependent way, whereas there was no significant reduction in Xcn1-treated HUVECs. Cycloheximide (CHX) was used as a positive control. Xcn2 at concentrations of 1000 and 3000 nM reduced the protein synthesis by more than 50%, which is comparable to the reduction evoked by CHX at 10 μg/ml (36 μM). Subsequently, we analyzed the impact of protein biosynthesis inhibition by Xcn2 on the protein levels of receptors that are crucially involved in the pro-inflammatory and pro-angiogenic activation of endothelial cells. After 6 h treatment with Xcn2, the protein level of TNF receptor 1 (TNFR1) was significantly and concentration-dependently reduced in HUVECs starting from a Xcn2 concentration of 100 nM (Fig. 6C). The decrease of the TNFR1 protein level by Xcn2 at a concentration of 1000 nM (Fig. S8A) was transient with onset at 2 h and disappearance at 18 h of treatment. At 3000 nM (Fig. S8B), however, Xcn2 led to a rapid loss of TNFR1 within 1 h, and a constant effect was observed after 6 h. Interestingly, mRNA expression of TNFR1 was significantly increased by Xcn2 (1000 nM) after 10 h of treatment and stayed constant at least for 24 h (Fig. S8C). Furthermore, the influence of Xcn2 on the protein level of another receptor that is of great importance for inflammatory processes, the interleukin 1 receptor type I (IL1R1), was evaluated (Fig. S8D). In contrast to the effect on TNFR1, Xcn2 did not alter IL1R1 total protein level.

Ultimately, we analyzed the influence of Xcn2 on prominent receptors that trigger pro-angiogenic siginaling events: VEGFR2, VEGFR1, FGFR1, and EGFR (Fig. 6D–G and Fig. S9). Xcn2 (1000 nM) caused a concentration-dependent reduction of the total protein levels of VEGFR2, VEGFR1, and FGFR1. The lowest concentration that evoked a significant effect was 100, 300, and 3000 nM for VEGFR2, VEGFR1, and FGFR1, respectively (Fig. 6D–F). This action was observed within an hour for both VEGFR2 and VEGFR1, which was not recovered for at least 24 h (Fig. S9A, B). The maximum effect on the protein level of FGFR1 was observed at 6 h (Fig. S9C). In contrast, Xcn2 did not reduce the protein level of EGFR after the compound was applied at concentrations up to 3000 nM for 24 h (Fig. 6G and Fig. S9D). Cycloheximide (CHX), a well-known eukaryotic protein synthesis inhibitor [29], was used as a positive control (Fig. S9).

4. Discussion

Discovering therapeutics with the ability to inhibit the uncontrolled inflammatory response, which causes self-damage of cells and consequently most human immunity-related disorders, is important to develop effective anti-inflammatory therapies [24]. The inflammatory response is a complex process that is orchestrated by many cellular interactions. In numerous severe diseases, inflammation and angiogenesis are engaged as co-dependent pathogenetic processes that share signaling pathways and molecules [30]. For example, in rheumatoid arthritis, infiltrated inflammatory cells generate an excess of angiogenic factors that facilitate the ingrowth of a vascular pannus over a joint surface [31]. These processes are strongly associated with the activation of vascular ECs, expressing CAMs, and presenting chemokines followed by the initiation of leukocyte migration from blood into the tissue [32].

In this study, we revealed for the first time that xenocoumacin (Xcn) 1 and 2, two natural products isolated from the nematode-associated bacterium *Xenorhabdus nematophila*, have the pharmacological activity to reduce inflammation- and angiogenesis-associated processes. Since their isolation and structure elucidation has been reported in 1991 [12], they have been widely investigated regarding their culture conditions and their activity as antimicrobial compounds [1,10]. The only emerging evidence for the biological effects of Xcns in mammalian cells was reported in the same study [12]: Both Xcns were shown to exhibit antiulcerogenic properties, i.e., they exerted beneficial actions on stress-induced gastric ulcers in rats after oral administration.

In the first step, we confirmed that both Xcns did not induce cytotoxic effects in ECs, in contrast to their well-known toxicity on prokaryotes and fungi [10]. Subsequently, we initially evaluated the ability of Xcns to impede the surface and total protein levels of ICAM-1, VCAM-1, and E-selectin, which are well-known to promote the recruitment of leukocytes [33]. Xcn2 was confirmed to markedly reduce these levels in response to both TNF and IL-1β cytokines under static and flow conditions. mRNA expression of ICAM and E-selectin was increased when ECs were treated with 1000 and 3000 nM Xcn2. Protein synthesis is not necessarily directly related to the mRNA levels, because many essential controls in gene expression occur at the translation level [34]. The increased mRNA levels might be due to compensate for the protein loss. Furthermore, the activation cascade of the proinflammatory transcription factor NF-κB was strongly affected by Xcn2: The compound inhibited various essential steps in the TNF-triggered pathway including p65 nuclear translocation, phosphorylation/activation of IKK-β and phosphorylation and degradation of IκBα. The total protein of TNFR1, which has a central role in the TNF-induced inflammation signaling [35], was also reduced up to 50%. Noteworthy, this result was similar to that of the well-known translation inhibitor cycloheximide [29]. Taken together, we have obtained comprehensive evidence for the inhibitory actions of Xcns on pro-inflammatory processes in endothelial cells, which indicate that Xcn2 exhibits superior activity compared to Xcn1 as suggested by the initial findings [12].

Macrophages, a specialized type of immune cells, are important players in inflammation that crucially participate in inflammation-associated tissue damage; however, drug-induced toxicity might cause an undesired hyper-responsive phenotype [15]. As a first step, we proceeded to our research by exploring the influence of Xcns on macrophage viability. Both Xcns exhibited pharmacological efficacy regarding the inhibition of proliferation at lower concentrations compared to ECs. Hence, concentration ranges defined by IC_{50} curves were used to evaluate the effect of Xcns on the pro-inflammatory response of macrophages. In RAW 264.7 macrophages, Xcn1 and 2 did not influence the LPS-induced levels of PGE_2 and COX-2 but reduced the levels of nitric oxide (NO) and the inducible NO synthase. Our findings suggest potent immunomodulating activities of Xcns on macrophages in addition to ECs.

Furthermore, we analyzed angiogenesis-related parameters in ECs, which have been considered as the major cell type reacting on angiogenic factors. Besides physiological processes, angiogenesis is an important step in the pathology of inflammation, which creates an inflammatory tissue abundant in blood vessels. It is also a key step in the growth and spread of malignant tumors, as well as in the progression of microvascular tissue in diabetes patients [36]. Concerning angiogenesis-related processes, we reveal for the first time that Xcn2 efficiently inhibits angiogenic processes in vitro. The compound decreased the proliferation, migration, angiogenic sprouting, and

network formation of human primary ECs and reduced the protein levels of important receptors that regulate angiogenesis, such as VEGFR2, VEGFR1, and FGFR1. Interestingly, the protein levels of EGFR, which represents another key regulator of angiogenesis, did not alter upon Xcn2 treatment for 24 h, suggesting that EGFR protein has a much longer half-life than the other receptors [23].

At this point, our final aim was to investigate whether Xcn2 impedes the protein synthesis in HUVECs. Recently, it was reported that amicoumacin A, which is structurally related to Xcns, inhibits protein synthesis in bacteria, yeast, and mammalian systems [37,38]. Therefore, we hypothesized that Xcn2 might affect protein biosynthesis in ECs and that this action might contribute to its observed in vitro anti-inflammatory action [34]. As hypothesized, our experiments prove that Xcn2 inhibits *de novo* protein synthesis, which is shown with an approximately 50% decrease in HUVECs. As was stated above, we observed a decrease in total protein levels of TNFR1 and VEGFR2, VEGFR1, and FGFR1. Xcn2-evoked protein biosynthesis inhibition could well be responsible for these results. Our data suggest that these receptors promptly vanish after the inhibition of protein biosynthesis. As described previously by our group [21,23], these proteins have quite short half-lives (in the range of 1–2 h) compared to down-stream signaling molecules, which explains the persistence of the total forms of proteins such as IκBα, IKK-β, Akt and Erk 1/2 after Xcn2 treatment. The cellular levels of the IL1R1 were also not influenced by Xcn2 or CHX indicating that this receptor has a much longer half-life than TNFR1.

In summary, this paper addresses the need for preclinical pharmacological characterization of Xcns in the context of inflammation and angiogenesis, so far lacking in the recent literature. Our biochemical and functional assays revealed the pharmacological potential of Xcn2 in inflammation/angiogenesis-associated processes, in vitro. The most remarkable result is that Xcn2 represents a potent inhibitor of protein synthesis in endothelial cells, which provides evidence for the rapid reduction of TNFR1, FGFR1 levels and the loss of VEGFR2 and VEGFR1 proteins in HUVECs. Furthermore, both the endothelial and the leukocytic side are influenced more in particular by Xcn2 during the inflammation-associated interaction of endothelial cells with leukocytes. Taken together, Xcn2 represents an interesting natural compound that exerts valuable pharmacological actions in vitro in the context of inflammatory and angiogenic processes. This potential warrants further evaluation in a preclinical setting.

Sources of funding

This work was supported by the Landesoffensive zur Entwicklung wissenschaftlich-ökonomischer Exzellenz (LOEWE) Center "Translational Biodiversity Genomics" (TBG).

Conflict of interest statement

The authors declare no commercial or financial conflicts of interest.

Acknowledgments

The authors are thankful to Isabell Franz and Mareike Lang for their technical support. We also thank G. Melissa Krishnathas for her help with the chemotaxis assay.

Appendix A. Supporting information

Supplementary data associated with this article can be found in the online version at doi:10.1016/j.biopha.2021.111765.

References

[1] E. Bode, A.K. Heinrich, M. Hirschmann, D. Abebew, Y.N. Shi, T.D. Vo, F. Wesche, Y. M. Shi, P. Grun, S. Simonyi, N. Keller, Y. Engel, S. Wenski, R. Bennet, S. Beyer, I. Bischoff, A. Buaya, S. Brandt, I. Cakmak, H. Cimen, S. Eckstein, D. Frank, R. Furst, M. Gand, G. Geisslinger, S. Hazir, M. Henke, R. Heermann, V. Lecaudey, W. Schafer, S. Schiffmann, A. Schuffler, R. Schwenk, M. Skaljac, E. Thines, M. Thines, T. Ulshofer, A. Vilcinskas, T.A. Wichelhaus, H.B. Bode, Promoter activation in deltahfq mutants as an efficient tool for specialized metabolite production enabling direct bioactivity testing, Angew. Chem. Int. Ed. Engl. 58 (52) (2019) 18957–18963, https://doi.org/10.1002/anie.201910563.

[2] O. Tyc, C. Song, J.S. Dickschat, M. Vos, P. Garbeva, The ecological role of volatile and soluble secondary metabolites produced by soil bacteria, Trends Microbiol. 25 (4) (2017) 280–292, https://doi.org/10.1016/j.tim.2016.12.002.

[3] S. Mushtaq, B.H. Abbasi, B. Uzair, R. Abbasi, Natural products as reservoirs of novel therapeutic agents, EXCLI J. 17 (2018) 420–451, https://doi.org/10.17179/excli2018-1174.

[4] V.J. Paul, S. Frautschy, W. Fenical, K.H. Nealson, Antibiotics in microbial ecology: Isolation and structure assignment of several new antibacterial compounds from the insect-symbiotic bacteriaXenorhabdus spp, J. Chem. Ecol. 7 (3) (1981) 589–597, https://doi.org/10.1007/BF00987707.

[5] G.O. Poinar, G. Thomas, M. Haygood, K.H. Nealson, Growth and luminescence of the symbolic bacteria associated with the terrestrial nematode, Heterorphabditis bacteriophora, Soil Biol. Biochem. 12 (1) (1980) 5–10, https://doi.org/10.1016/0038-0717(80)90095-4.

[6] G.M. Thomas, G.O. Poinar, Xenorhabdus gen-nov, a genus of entomopathogenic, nematophilic bacteria of the family enterobacteriaceae, Int. J. Syst. Bacteriol. 29 (4) (1979) 352–360, https://doi.org/10.1099/00207713-29-4-352.

[7] H.B. Park, C.E. Perez, E.K. Perry, J.M. Crawford, Activating and attenuating the amicoumacin antibiotics, Molecules 21 (7) (2016), https://doi.org/10.3390/molecules21070824.

[8] D. Park, K. Ciezki, R. van der Hoeven, S. Singh, D. Reimer, H.B. Bode, S. Forst, Genetic analysis of xenocoumacin antibiotic production in the mutualistic bacterium Xenorhabdus nematophila, Mol. Microbiol. 73 (5) (2009) 938–949, https://doi.org/10.1111/j.1365-2958.2009.06817.x.

[9] Y.M. Shi, H.B. Bode, Chemical language and warfare of bacterial natural products in bacteria-nematode-insect interactions, Nat. Prod. Rep. 35 (4) (2018) 309–335, https://doi.org/10.1039/c7np00054e.

[10] S. Guo, S. Zhang, X. Fang, Q. Liu, J. Gao, M. Bilal, Y. Wang, X. Zhang, Regulation of antimicrobial activity and xenocoumacins biosynthesis by pH in Xenorhabdus nematophila, Micro Cell Fact. 16 (1) (2017) 203, https://doi.org/10.1186/s12934-017-0813-7.

[11] B.V. Mc Inerney, W.C. Taylor, The xenocoumarins and related biologically active dihydroisocoumarins, in: R. Atta ur (Ed.), Studies in Natural Products Chemistry, Elsevier, 1995, pp. 381–422, https://doi.org/10.1016/S1572-5995(06)80138-9.

[12] B.V. McInerney, W.C. Taylor, M.J. Lacey, R.J. Akhurst, R.P. Gregson, Biologically active metabolites from Xenorhabdus spp., part 2. Benzopyran-1-one derivatives with gastroprotective activity, J. Nat. Prod. 54 (3) (1991) 785–795, https://doi.org/10.1021/np50075a006.

[13] L. Chen, H. Deng, H. Cui, J. Fang, Z. Zuo, J. Deng, Y. Li, X. Wang, L. Zhao, Inflammatory responses and inflammation-associated diseases in organs, Oncotarget 9 (6) (2017) 7204–7218, https://doi.org/10.18632/oncotarget.23208.

[14] S. Krishnamoorthy, K.V. Honn, Inflammation and disease progression, Cancer Metastas. Rev. 25 (3) (2006) 481–491, https://doi.org/10.1007/s10555-006-9016-0.

[15] J. Kalucka, L. Bierhansl, B. Wielockx, P. Carmeliet, G. Eelen, Interaction of endothelial cells with macrophages—linking molecular and metabolic signaling, Pflüg. Arch. Eur. J. Physiol. 469 (3) (2017) 473–483, https://doi.org/10.1007/s00424-017-1946-6.

[16] D. Reimer, E. Luxenburger, A.O. Brachmann, H.B. Bode, A new type of pyrrolidine biosynthesis is involved in the late steps of xenocoumacin production in Xenorhabdus nematophila, ChemBioChem 10 (12) (2009) 1997–2001, https://doi.org/10.1002/cbic.200900187.

[17] E.A. Jaffe, R.L. Nachman, C.G. Becker, C.R. Minick, Culture of human endothelial cells derived from umbilical veins. Identification by morphologic and immunologic criteria, J. Clin. Invest. 52 (11) (1973) 2745–2756, https://doi.org/10.1172/JCI107470.

[18] I. Nicoletti, G. Migliorati, M.C. Pagliacci, F. Grignani, C. Riccardi, A rapid and simple method for measuring thymocyte apoptosis by propidium iodide staining and flow cytometry, J. Immunol. Methods 139 (2) (1991) 271–279, https://doi.org/10.1016/0022-1759(91)90198-o.

[19] R. Ingelfinger, M. Henke, L. Roser, T. Ulshofer, A. Calchera, G. Singh, M. J. Parnham, G. Geisslinger, R. Furst, I. Schmitt, S. Schiffmann, Unraveling the pharmacological potential of lichen extracts in the context of cancer and inflammation with a broad screening approach, Front. Pharm. 11 (1322) (2020) 1322, https://doi.org/10.3389/fphar.2020.01322.

[20] B. Ma, M. Li, S. Fuchs, I. Bischoff, A. Hofmann, R.E. Unger, C.J. Kirkpatrick, Short-term hypoxia promotes vascularization in co-culture system consisting of primary human osteoblasts and outgrowth endothelial cells, J. Biomed. Mater. Res. Part A 108 (1) (2020) 7–18, https://doi.org/10.1002/jbm.a.36786.

[21] A. Stark, R. Schwenk, G. Wack, G. Zuchtriegel, M.G. Hatemler, J. Brautigam, A. Schmidtko, C.A. Reichel, I. Bischoff, R. Furst, Narciclasine exerts anti-inflammatory actions by blocking leukocyte-endothelial cell interactions and down-regulation of the endothelial TNF receptor 1, FASEB J. 33 (8) (2019) 8771–8781, https://doi.org/10.1096/fj.201802440R.

[22] G. Cotter, E. Kaluski, A. Blatt, O. Milovanov, Y. Moshkovitz, R. Zaidenstein, A. Salah, D. Alon, Y. Michovitz, M. Metzger, Z. Vered, A. Golik, L-NMMA (a nitric oxide synthase inhibitor) is effective in the treatment of cardiogenic shock, Circulation 101 (12) (2000) 1358–1361, https://doi.org/10.1161/01.cir.101.12.1358.

[23] J. Brautigam, I. Bischoff, C. Schurmann, G. Buchmann, J. Epah, S. Fuchs, E. Heiss, R.P. Brandes, R. Furst, Narciclasine inhibits angiogenic processes by activation of Rho kinase and by downregulation of the VEGF receptor 2, J. Mol. Cell Cardiol. 135 (2019) 97–108, https://doi.org/10.1016/j.yjmcc.2019.08.001.
[24] W.A. Muller, Leukocyte-endothelial cell interactions in the inflammatory response, Lab. Invest. 82 (5) (2002) 521–533, https://doi.org/10.1038/labinvest.3780446.
[25] A. Deptala, E. Bedner, W. Gorczyca, Z. Darzynkiewicz, Activation of nuclear factor kappa B (NF-kappaB) assayed by laser scanning cytometry (LSC), Cytometry 33 (3) (1998) 376–382, https://doi.org/10.1002/(sici)1097-0320(19981101)33:3<376::aid-cyto13>3.0.co;2-q.
[26] T. Lawrence, The nuclear factor NF-kappaB pathway in inflammation, Cold Spring Harb. Perspect. Biol. 1 (6) (2009), 001651, https://doi.org/10.1101/cshperspect.a001651.
[27] P.R. Somanath, O.V. Razorenova, J. Chen, T.V. Byzova, Akt1 in endothelial cell and angiogenesis, Cell Cycle 5 (5) (2006) 512–518, https://doi.org/10.4161/cc.5.5.2538.
[28] R. Srinivasan, T. Zabuawala, H. Huang, J. Zhang, P. Gulati, S. Fernandez, J. C. Karlo, G.E. Landreth, G. Leone, M.C. Ostrowski, Erk1 and Erk2 regulate endothelial cell proliferation and migration during mouse embryonic angiogenesis, PLoS One 4 (12) (2009) 8283, https://doi.org/10.1371/journal.pone.0008283.
[29] T. Schneider-Poetsch, J. Ju, D.E. Eyler, Y. Dang, S. Bhat, W.C. Merrick, R. Green, B. Shen, J.O. Liu, Inhibition of eukaryotic translation elongation by cycloheximide and lactimidomycin, Nat. Chem. Biol. 6 (3) (2010) 209–217, https://doi.org/10.1038/nchembio.304.
[30] D. Aguilar-Cazares, R. Chavez-Dominguez, A. Carlos-Reyes, C. Lopez-Camarillo, O. N. Hernadez de la Cruz, J.S. Lopez-Gonzalez, Contribution of angiogenesis to inflammation and cancer, Front. Oncol. 9 (1399) (2019) 1399, https://doi.org/10.3389/fonc.2019.01399.
[31] S.Y. Yoo, S.M. Kwon, Angiogenesis and its therapeutic opportunities, Mediat. Inflamm. 2013 (2013), 127170, https://doi.org/10.1155/2013/127170.
[32] J. Middleton, L. Americh, R. Gayon, D. Julien, L. Aguilar, F. Amalric, J.-P. Girard, Endothelial cell phenotypes in the rheumatoid synovium: activated, angiogenic, apoptotic and leaky, Arthritis Res. Ther. 6 (2) (2004) 60–72, https://doi.org/10.1186/ar1156.
[33] V. Tisato, G. Zauli, E. Rimondi, S. Gianesini, L. Brunelli, E. Menegatti, P. Zamboni, P. Secchiero, Inhibitory effect of natural anti-inflammatory compounds on cytokines released by chronic venous disease patient-derived endothelial cells, Mediat. Inflamm. 2013 (2013), 423407, https://doi.org/10.1155/2013/423407.
[34] J. Liu, Y. Xu, D. Stoleru, A. Salic, Imaging protein synthesis in cells and tissues with an alkyne analog of puromycin, Proc. Natl. Acad. Sci. U.S.A. 109 (2) (2012) 413–418, https://doi.org/10.1073/pnas.1111561108.
[35] J.S. Pober, Endothelial activation: intracellular signaling pathways, Arthritis Res. 4 (Suppl 3) (2002) S109–S116, https://doi.org/10.1186/ar576.
[36] F. Mor, F.J. Quintana, I.R. Cohen, Angiogenesis-inflammation cross-talk: vascular endothelial growth factor is secreted by activated T cells and induces Th1 polarization, J. Immunol. 172 (7) (2004) 4618–4623, https://doi.org/10.4049/jimmunol.172.7.4618.
[37] Y.S. Polikanov, I.A. Osterman, T. Szal, V.N. Tashlitsky, M.V. Serebryakova, P. Kusochek, D. Bulkley, I.A. Malanicheva, T.A. Efimenko, O.V. Efremenkova, A. L. Konevega, K.J. Shaw, A.A. Bogdanov, M.V. Rodnina, O.A. Dontsova, A. S. Mankin, T.A. Steitz, P.V. Sergiev, Amicoumacin a inhibits translation by stabilizing mRNA interaction with the ribosome, Mol. Cell 56 (4) (2014) 531–540, https://doi.org/10.1016/j.molcel.2014.09.020.
[38] I.V. Prokhorova, K.A. Akulich, D.S. Makeeva, I.A. Osterman, D.A. Skvortsov, P. V. Sergiev, O.A. Dontsova, G. Yusupova, M.M. Yusupov, S.E. Dmitriev, Amicoumacin A induces cancer cell death by targeting the eukaryotic ribosome, Sci. Rep. 6 (2016) 27720, https://doi.org/10.1038/srep27720.